journal

J. Am. Ceram. Soc., 89 [6] 1840–1846 (2006)
DOI: 10.1111/j.1551-2916.2006.01014.x


# Phase Behavior, 3-D Structure, and Rheology of Colloidal Microsphere–Nanoparticle Suspensions

Summer K. Rhodes and Jennifer A. Lewis**,†

Materials Science and Engineering Department, University of Illinois Urbana-Champaign, Urbana, Illinois 61801

**A new route for tailoring the behavior of colloidal suspensions through nanoparticle additions is reviewed. Specifically, the interparticle interactions, phase behavior, 3-D structure, and rheological properties of microsphere–nanoparticle mixtures that possess both high charge and size asymmetry are described. Negligibly charged microspheres, which flocculate when suspended alone, undergo a remarkable stabilizing transition upon the addition of highly charged nanoparticles. The formation of a dynamic nanoparticle halo around each colloid induces an effective repulsion between the microspheres that promotes their stability. With increasing nanoparticle concentration, the colloids again undergo flocculation because of the emergence of an effective microsphere attraction, whose magnitude exhibits a quadratic dependence on nanoparticle volume fraction. The broader impact of these observations on colloidal stabilization and assembly of advanced ceramics is highlighted.**

## I. Introduction

Colloidal processing offers the potential to reliably produce ceramic films and bulk forms through careful control of initial suspension "structure" and its evolution during fabrication.[1–5] This is achieved by mitigating the ubiquitous van der Waals forces that lead to particle flocculation via electrostatic, steric, or other repulsive interactions. A common strategy is to induce charge on the colloid surface by altering the composition of the solution in which they are suspended. Both the magnitude and range of the electrostatic repulsion between colloidal species can be tuned by adding acid, base, or electrolyte species. Another common strategy involves the addition of organic dispersants that strongly adsorb onto ceramic particle surfaces. In this case, the magnitude and range of the steric repulsion can be controlled by tailoring the adlayer density and thickness as well as the solvent quality. Recently, a new strategy has been introduced that involves the use of highly charged nanoparticles to regulate the stability of colloidal suspensions in which they dwell. This mechanism, referred to as nanoparticle haloing,[6,7] has been observed in binary mixtures that possess both high size and charge asymmetry, in which the colloidal microspheres are negligibly charged and the nanoparticles are highly charged.

It is well known that non-adsorbing and strongly adsorbing nanoparticle species can alter colloidal stability via entropic depletion interactions[8–11] or heteroflocculation,[12–16] respectively. The term "depletion" describes the exclusion of these smaller species from the gap region between colloidal particles that arises when the colloid separation distance becomes less than the characteristic nanoparticle size. The resulting concentration gradient between the gap region and bulk solution gives rise to an attractive force, whose magnitude scales with the volume fraction of smaller species, their charge, and the size ratio of large to small species.[8,11,17] Heteroflocculation ensues when oppositely charged nanoparticles strongly adsorb onto colloid surfaces. At low surface coverage, the adsorbed nanoparticles serve as bridging flocculants, whereas restabilization due to charge reversal can occur at higher surface coverage. Recent experimental,[6,7,13,18] theoretical,[19–22] and simulation[23,24] efforts suggest that charged nanoparticles in solution can affect colloidal stability through other self-organizing pathways. For example, charged nanoparticles are predicted to segregate to regions surrounding large uncharged colloids forming a "halo" especially in systems with high size asymmetry in which the ratio of small to large spheres is also high.[20,22–24] This segregation can be driven either by a weak electrostatic attraction between the large and small particles[23,24] or by an electrostatic repulsion between smaller species in solution.[22]

Here, we review the fundamental behavior of microsphere–nanoparticle mixtures, whose interactions, phase behavior, structure, and properties are regulated by the formation of nanoparticle halos. We begin by describing the interparticle interactions between microsphere–microsphere, nanoparticle–nanoparticle, and microsphere–nanoparticle species in a system comprised of negligibly charged, silica microspheres and positively charged, hydrous zirconia nanoparticles in water. Next, we describe the phase behavior observed as a function of varying microsphere and nanoparticle concentration in both aqueous and index-matched, glycerol–water solutions. Following this, we present direct images of colloidal phases assembled from these mixtures in an index-matched solution acquired by confocal microscopy. We then show how the rheological properties of these binary suspensions can be varied over a broad range through nanoparticle additions. Finally, we highlight the potential impact of this new stabilization route on the colloidal assembly of ceramics and other materials.

## II. Microsphere–Nanoparticle Interactions

The interparticle interactions for a binary system comprised of silica microspheres and hydrous zirconia nanoparticles suspended in water (pH 1.5) are calculated using the well-known DLVO (Derjaguin–Landau–Verwey–Overbeek) theory.[25,26]

$$V_{\text{total}}(h) = V_{\text{vdW}}(h) + V_{\text{elect}}(h) \tag{1}$$

The van der Waals (vdW) potential between identical spheres is given by

$$V_{\text{vdW}}(h) = \frac{-A_{131}(h)}{6}\left[\frac{2}{s^2-4} + \frac{2}{s^2} + \ln\left(\frac{s^2-4}{s^2}\right)\right] \tag{2}$$

with

$$S = \frac{2a+h}{a} \tag{3}$$

G. Messing—contributing editor

Manuscript No. 21340. Received January 6, 2006; approved January 28, 2006.
Supported by the U.S. Department of Energy, Division of Materials Science under Award No. DEFG02-91ER45439 through the Frederick Seitz Materials Research Laboratory at the University of Illinois at Urbana-Champaign. S. K. Rhodes is supported by an NSF Graduate Fellowship.
Presented at the 9th International Ceramic Processing Science Symposium, Coral Springs, FL, Jan. 8–11, 2006.
**Fellow, American Ceramic Society.
†Author to whom correspondence should be addressed. e-mail: jalewis@uiuc.edu

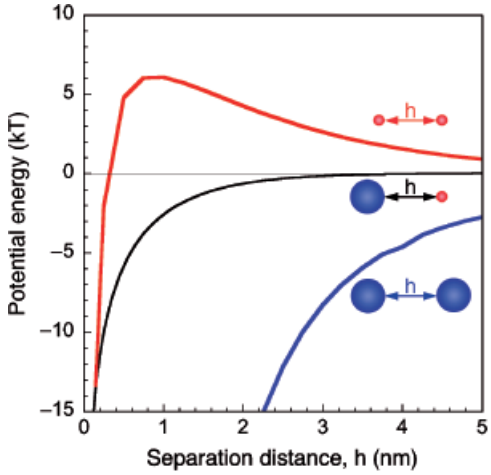


**Fig. 1.** Interparticle potential energy as a function of separation distance between microspheres (blue) of radius, $a_{micro}$ 590 nm, nanoparticles (red) of radius, $a_{nano}$ 3 nm, and a microsphere–nanoparticle pair (black) in aqueous solution (pH 1.5).

and $A_{131}(h)$ as the distance-dependent Hamaker value for spheres of radius, $a$ ($a_{micro} = 590$ nm, $a_{nano} = 3$ nm) and separation distance, $h$ (see Prieve and Russel[27] for details). The electrostatic double-layer interactions are modeled using the Hogg–Healy–Fuerstenau expression.[28,29] For two nanoparticles at a surface separation $h$, this equation, under constant-potential conditions, reduces to an exponentially decaying repulsive interaction,[26]

$$\begin{aligned} V_{elect}^{nano} &= \varepsilon_0\varepsilon_r\pi\sigma_{nano}\Psi_{nano}^2 \ln[1+\exp(-\kappa h)] \\ &\approx \varepsilon_0\varepsilon_r\pi\sigma_{nano}\Psi_{nano}^2 \exp(-\kappa h) \end{aligned} \quad (4)$$

where the approximation is valid for $\kappa h \gg 1$. $\Psi_{nano}$ is taken to be the nanoparticle zeta potential ($\zeta_{nano} \sim 70$ mV), $\kappa$ the inverse screening length (2 nm in aqueous solution), $\varepsilon_0$ the vacuum permittivity, and $\varepsilon_r$ the dielectric constant of the solvent (80 for water). As the silica microspheres are negligibly charged ($\zeta_{micro} \sim 1$ mV), we ignore the electrostatic interaction between them. However, an electrostatic double-layer interaction arises between the microspheres and nanoparticles, which for large size asymmetry is described by[28]

$$\begin{aligned} V_{elect}^{micro-nano} &= \tfrac{1}{2}\varepsilon_0\varepsilon_r\pi\sigma_{nano}\Psi_{nano}^2 \ln[1-\exp(-2\kappa h)] \\ &\approx -\tfrac{1}{2}\varepsilon_0\varepsilon_r\pi\sigma_{nano}\Psi_{nano}^2 \exp(-2\kappa h) \end{aligned} \quad (5)$$

where the approximation is again valid for $\kappa h \gg 1$. The interparticle potentials calculated between microsphere, nanoparticle, and microsphere–nanoparticle pairs are shown in Fig. 1. The microsphere interactions are dominated by a van der Waals attraction, whereas the nanoparticles electrostatically repel one another due to their high charge. Interestingly, an electrostatic attraction is induced between microsphere–nanoparticle species, which promotes the formation of a nanoparticle halo around each colloid.[22,23]

To quantify the degree of association, or haloing, between the microsphere–nanoparticle species in this system, the effective microsphere $\zeta$ potential, $\zeta_{micro}$, and nanoparticle adsorption are measured as a function of nanoparticle volume fraction, $\phi_{nano}$. The zeta potential of the microspheres in the absence of nanoparticles is 1 mV. With increasing $\phi_{nano}$ the effective $\zeta_{micro}$ increased to $\sim$65 mV at $\phi_{nano}$ of 0.003 (Fig. 2). The extent of nanoparticle adsorption on the silica microsphere surfaces is also plotted in Fig. 2 as a function of nanoparticle concentration in solution. A significant fraction of the nanoparticle species remain in the bulk solution, even at the lowest nanoparticle concentrations studied, indicating that strong nanoparticle

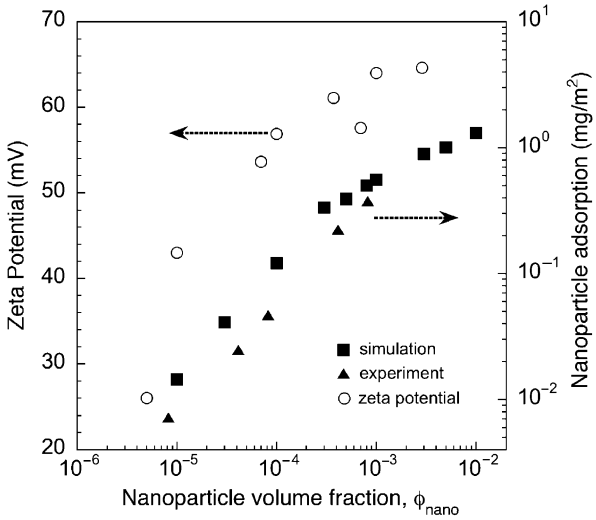


**Fig. 2.** Plot of the effective microsphere zeta potential ($\phi_{micro} = 10^{-3}$) and nanoparticle adsorption on silica microspheres ($\phi_{micro} = 0.10$) as a function of $\phi_{nano}$ in aqueous solution (pH 1.5), as measured experimentally and through simulation.

adsorption is unlikely. These data are in good agreement with results from simulations recently reported by Liu and Luijten,[23,24] which are superimposed in Fig. 2.

Monte Carlo simulations have been carried out to determine the effective microsphere interaction potential induced as a function of nanoparticle volume fraction in these binary mixtures.[18,23,24] Figure 3 shows the effective microsphere potential $V_{eff}/k_BT$ calculated from the colloidal pair correlation function obtained in the simulations. Colloidal many-body effects have

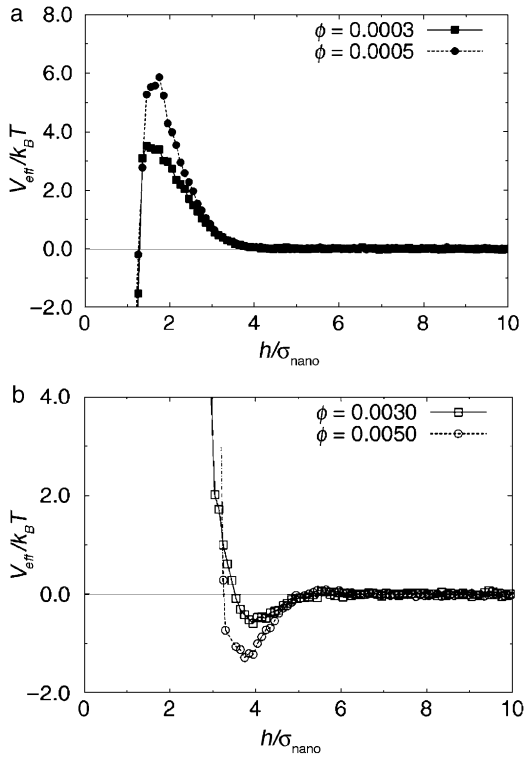


**Fig. 3.** Effective potential $V_{eff}/k_BT$ between microspheres suspended in an aqueous solution, as a function of the surface-to-surface separation, $h$ (in units of nanoparticle diameter $\sigma_{nano}$). (a) At low nanoparticle volume fraction, a repulsive barrier arises that increases with $\phi_{nano}$. (b) At higher nanoparticle volume fraction, an attractive minimum appears as well, with a strength that increases with increasing $\phi_{nano}$. [Reprinted with permission from Martinez *et al.*[18] Copyright 2005 American Chemical Society].

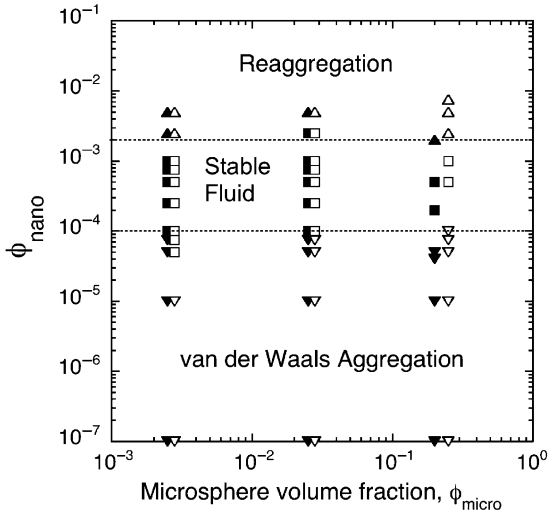


**Fig. 4.** Log–log plot of the phase behavior of microsphere–nanoparticle mixtures in both aqueous (filled symbols) and index matched (open symbols) systems. [Reprinted with permission from Martinez *et al.*[18] Copyright 2005 American Chemical Society.]

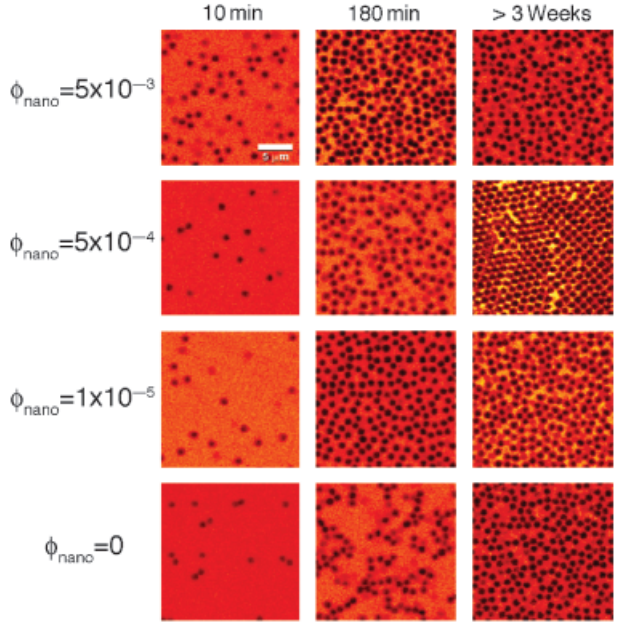


**Fig. 5.** Confocal images ($x$–$y$ scans) acquired at the sediment-substrate interface as a function of sedimentation time for colloidal phases assembled from binary mixtures comprised of $\phi_{micro} = 2.5 \times 10^{-3}$ and varying $\phi_{nano}$ in an index-matched solution.[18]

been eliminated by performing these simulations in the dilute colloid limit. At low nanoparticle concentrations in water (Fig. 3(a)), a repulsive barrier appears that increases with nanoparticle volume fraction. At intermediate nanoparticle concentration (Fig. 3(b)), an attractive minimum appears in the potential, preceding the repulsive barrier. It was found by Luijten and Liu[23] that the depth of this minimum grows quadratically with $\phi_{nano}$, indicating a qualitative difference with the linear concentration dependence exhibited by regular depletion interactions.[8,30] Examination of microsphere–nanoparticle configurations indicates that, upon approach of two microspheres, the halos remain largely unperturbed, and at a separation corresponding to the attractive minimum of the effective potential only limited nanoparticle depletion is observed in the region between the opposing halos. Based on this analysis, one would expect the phase behavior, structure, and rheological properties of these binary mixtures to exhibit a strong dependence on nanoparticle concentration.

## III. Phase Behavior of Microsphere–Nanoparticle Mixtures

The phase behavior of microsphere–nanoparticle mixtures of varying composition in both aqueous and index-matched solutions is shown in Fig. 4. In the absence of nanoparticles, negligibly-charged silica microspheres flocculate owing to van der Waals interactions yielding clusters that settle rapidly to form a dense, amorphous sediment. Below a lower critical nanoparticle volume fraction $\phi^{L,C}$, the system remains unstable, yielding a dense, amorphous sediment. This observation suggests that the microsphere interactions are indeed influenced by van der Waals forces, even in index-matched systems where they are substantially weakened. However, these forces decay very rapidly with increasing microsphere separation and the nanoparticle-induced repulsive barrier, as demonstrated in Fig. 3(a), is sufficient to prevent aggregation. Indeed, at intermediate nanoparticle volume fractions ($\phi^{L,C} \leq \phi_{nano} < \phi^{U,C}$), the system resides in the stable fluid region from which individual colloidal microspheres settle under gravity to produce a crystalline sediment. The value of $\phi^{L,C}$ appears to be relatively insensitive to microsphere volume fraction or the solution in which they interact. Finally, above the upper critical volume fraction ($\phi_{nano} \geq \phi^{U,C}$), the system becomes unstable, once again yielding an amorphous structure upon sedimentation. This is consistent with the attractive minima observed in the simulations (Fig. 3(b)) at higher nanoparticle concentrations.

## IV. 3-D Structure of Colloidal Phases Assembled from Microsphere–Nanoparticle Mixtures

The structural evolution observed during gravity-driven assembly of colloidal microspheres from index-matched binary mixtures can be monitored in situ using confocal microscopy. The use of an index-matched, glycerol–water solution is needed to facilitate 3-D imaging of the colloidal structures formed. We present the time evolution sequence for binary mixtures at a low initial microsphere volume fraction ($\phi_{micro} = 2.5 \times 10^{-3}$), because the dynamics at higher concentrations are too fast to capture. The $x$–$y$ scans, shown in Fig. 5, reveal the dramatic differences in structure observed for binary mixtures assembled from four different regions within the phase diagram (see Fig. 4), where $\phi_{nano} = 0$ (microspheres only), $10^{-5}$ (lower unstable region), $5 \times 10^{-4}$ (stable fluid region), and $5 \times 10^{-3}$ (upper unstable region). In these images, the colloidal microspheres appear as dark circular features against a lighter background that corresponds to the index-matched, fluorescent dyed solution. In the absence of nanoparticle additions, the microspheres aggregate into string-like clusters that are elongated in shape. This type of cluster formation leads to an initially open sediment structure, as shown in the $x$–$z$ scan depicted in Fig. 6. However, this amorphous sediment will ultimately densify over time under its own weight, as microspheres continue to settle from solution. In sharp contrast, there is little evidence of cluster formation in binary mixtures that reside in the lower unstable region ($\phi_{nano} = 10^{-5}$). Despite being unable to visualize microsphere clusters in this sample, we observe that they exhibit a faster sedimentation rate than individual microspheres settling from the stable fluid phase ($\phi_{nano} = 5 \times 10^{-4}$). This is perhaps most obvious in the $x$–$y$ scans acquired at 180 min, in which there is a greater accumulation of colloidal microspheres at the substrate–sediment interface for the unstable mixture. A finite number of small clusters must form in mixtures that reside in the lower unstable region—otherwise, there would be no difference in the rate of microsphere accumulation relative to the settling rate observed for individual microspheres in the stable region. This is confirmed by bulk sedimentation results (see Fig. 7(a)) that reveal significantly higher settling velocities and lower sediment volume fractions for microspheres in mixtures that reside in the lower (and upper) unstable regions than for those in the stable fluid phase. Finally, in the upper unstable region

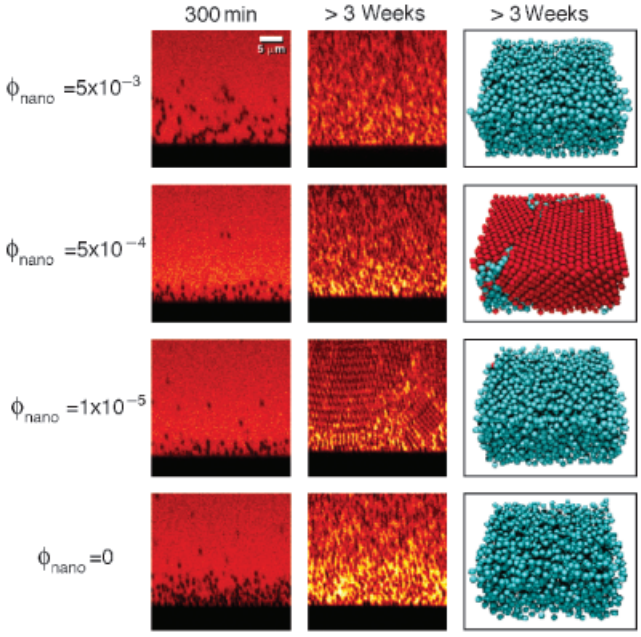


**Fig. 6.** Confocal images ($x$–$z$ scans) acquired from colloidal phases assembled from binary mixtures comprised of $\phi_{micro} = 2.5 \times 10^{-3}$ and varying $\phi_{nano}$ at different sedimentation times along with 3-D reconstructions of these structures with the microspheres color-coded to distinguish colloidal particles in disordered (blue) and crystalline regions (red) (>3 weeks of settling).[18]

($\phi_{nano} = 5 \times 10^{-3}$), there is again visual evidence in both the $x$–$y$ and $x$–$z$ scans that the microspheres form clusters, albeit far more compact in nature than those formed in the absence of nanoparticle additions. In this region, the microsphere clusters settle from suspension to form an amorphous sediment that is initially more open than that formed from either of the other mixtures, but denser than that produced in the absence of added nanoparticles.

At the longest times probed (>3 weeks), only colloids assembled from the stable fluid phase are observed to crystallize. In all other cases, the final sediments consist of a dense, amorphous structure. This is illustrated nicely by the 3-D reconstructions shown in Fig. 6. The microspheres are color-coded to distinguish colloidal particles in disordered (blue) and crystalline regions (red). Crystalline structures are observed only for samples that settle from binary mixture that reside in the stable fluid region. The 3-D reconstructions reveal the polycrystalline nature of sediments formed from within this region, with blue particles highlighting domain boundaries that exist at the interface between single crystal domains. Outside this region, the sediments are comprised of dense, amorphous structures (or gels).

## V. Rheological Properties of Microsphere–Nanoparticle Mixtures

The flow behavior of microsphere–nanoparticle mixtures reflects the profound structural variations in the phases described above. The apparent viscosity as a function of shear rate for microsphere–nanoparticle mixtures are shown in Fig 8(a). In the absence of nanoparticles, the colloidal microsphere suspension exhibits a low shear viscosity of roughly 400 Pa·s and strong shear thinning behavior characteristic of a flocculated system. Both the viscosity and degree of shear thinning decrease dramatically with increasing nanoparticle volume fraction. Suspensions prepared within the homogeneous fluid phase, where $\phi^{L,C} \leq \phi_{nano} < \phi^{U,C}$, exhibit an apparent viscosity of ~0.004 Pa·s—which is several orders of magnitude below the flocculated mixtures. As expected, these fully stabilized suspensions also exhibit Newtonian flow behavior. At $\phi_{nano} \geq \phi^{U,C}$, the mixtures reflocculate as evidenced by an increase in their apparent viscosity and degree of shear thinning. For example,

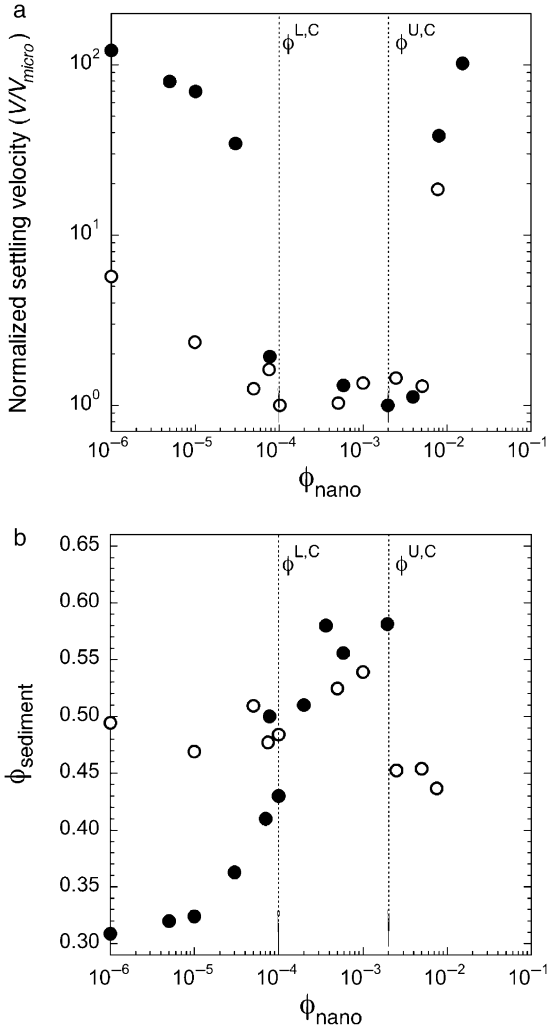


**Fig. 7.** (a) Normalized initial settling velocity ($V/V_{micro}$) and (b) sediment volume fraction ($\phi_{sediment}$) as a function of nanoparticle volume fraction ($\phi_{nano}$) for structures assembled from binary mixtures ($\phi_{micro} = 0.1$) in an aqueous solution (filled symbols) and index-matched solution (open symbols).[18]

when $\phi_{nano}$ was nearly double the value of $\phi^{U,C}$, the low shear suspension viscosity was two orders of magnitude higher than that observed for the fully stabilized suspensions.

Oscillatory measurements were carried out on microsphere–nanoparticle mixtures residing in the lower gel ($\phi_{nano} < \phi^{L,C}$), fluid ($\phi^{L,C} \leq \phi_{nano} < \phi^{U,C}$), and upper gel ($\phi_{nano} \geq \phi^{U,C}$) phase regions. The elastic modulus ($G'$) of mixtures of fixed microsphere volume fraction ($\phi_{micro} = 0.45$) display a strong dependence on nanoparticle volume fraction ($\phi_{nano}$), as shown in Fig. 8(b). The dashed lines denote the observed boundaries between the three phases based on bulk sedimentation rates for $\phi_{micro} = 0.45$. In the absence of nanoparticles, concentrated microsphere gels exhibit a $G'$ of 50 000–60 000 Pa. Within the lower aggregated phase, the value of $G'$ decreases by more than three orders of magnitude as $\phi_{nano}$ approaches $\phi^{L,C}$. In contrast, mixtures residing in the upper gel phase exhibit the opposite dependence of $G'$ on $\phi_{nano}$. In this region, $G'$ is observed to gradually increase as $\phi_{nano}$ increases beyond $\phi^{U,C}$. As expected, microsphere–nanoparticle mixtures residing in the homogeneous fluid phase exhibit the lowest values of $G'$, on the order of a few Pa.

## VI. Current Perspective

Recent experimental work by Chan and Lewis[13] and others[6,7,18] has demonstrated the generality of nanoparticle haloing as a

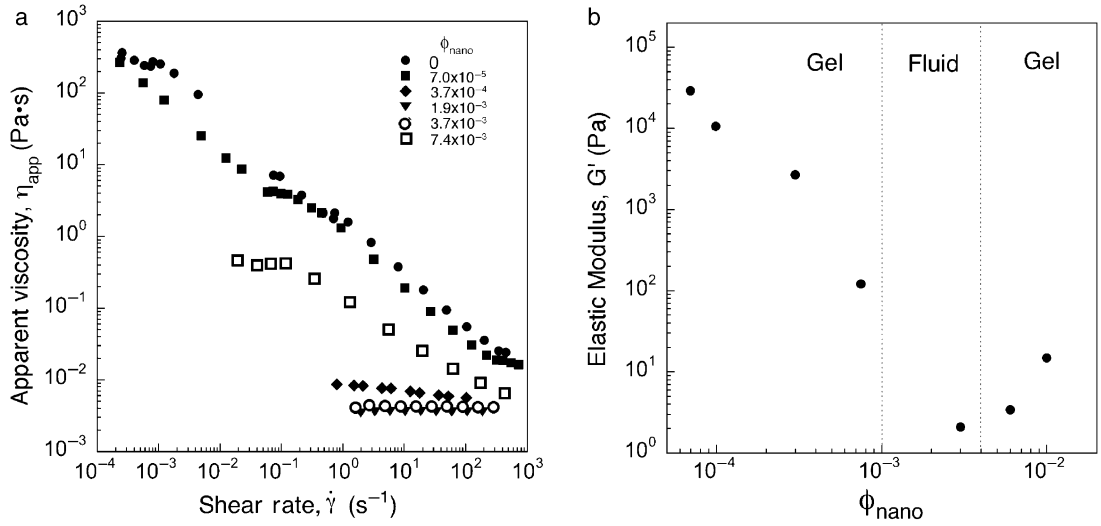


**Fig. 8.** (a) Log–log plot of apparent viscosity ($\eta_{app}$) as a function of shear rate ($\gamma$) for microsphere–nanoparticle mixtures at constant microsphere volume fraction ($\phi_{micro} = 0.30$ and $a_{micro} = 285$ nm) and varying $\phi_{nano}$ and (b) log–log plot of elastic modulus ($G'$) at constant $\phi_{micro} = 0.45$.[7]

novel colloid stabilization mechanism. For example, Chan and Lewis[13] studied the behavior of binary mixtures comprised of silica microspheres and polystyrene nanoparticles, whose mutual electrostatic interactions could be tuned by varying the solution pH and nanoparticle surface functionalization. Specifically, three binary mixtures were investigated, strongly attractive, weak (haloing), and strongly repulsive, as classified by their microsphere–nanoparticle interactions. Important differences in system behavior emerged, which depended on both the initial microsphere stability and whether the added nanoparticles served as bridging, haloing, or depletant species, respectively.[13] They found that negligibly charged silica microspheres could be stabilized by highly negatively charged polystyrene nanoparticles, as shown in both sedimentation studies and direct imaging of the assembled colloidal phases. The similarity in behavior observed for this model system and that of the silica microsphere–hydrous zirconia nanoparticle mixtures described above was considered to be strong evidence of a common stabilization mechanism, namely nanoparticle haloing.

Kong *et al.*[31] investigated the stabilization of aqueous alumina suspensions by silica sols under solution conditions where the alumina colloids are negligibly charged and the silica nanoparticle are highly negatively charged. By probing the sedimentation and rheological properties, they observed a remarkable stabilizing transition above a critical nanoparticle concentration. They attributed this to nanoparticle haloing based on direct and indirect measurements that revealed a limited extent of association between the alumina colloids and silica nanoparticles in

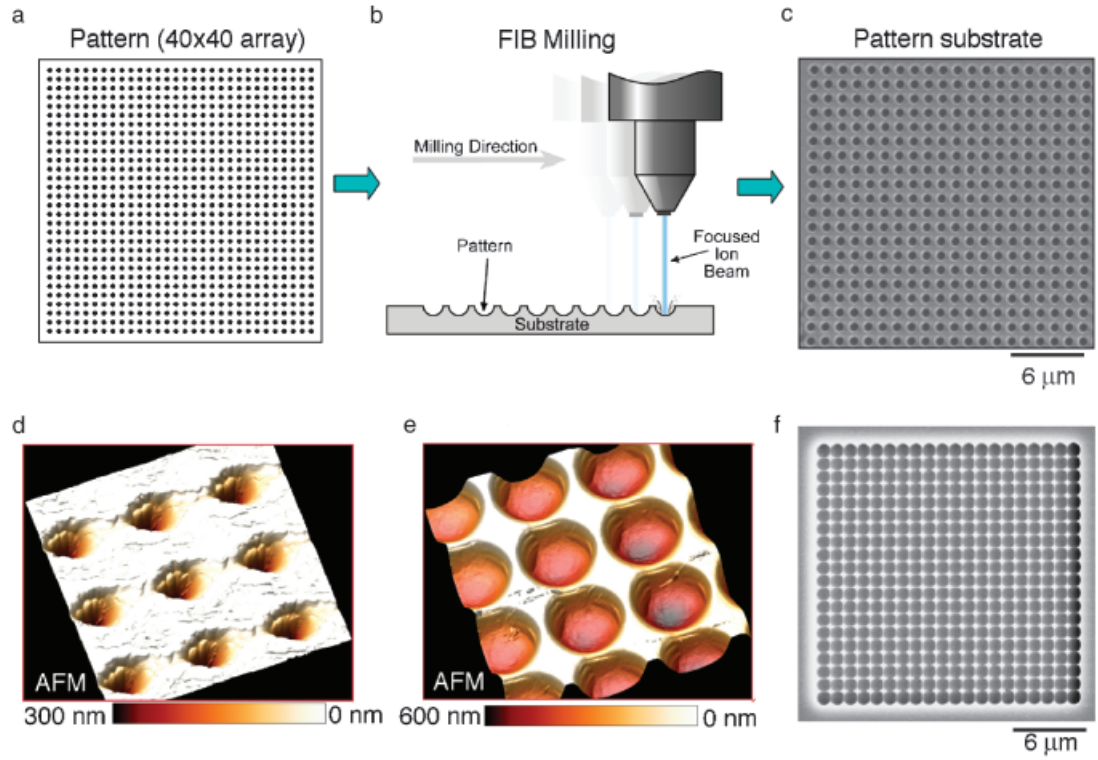


**Fig. 9.** Fabrication of patterned glass substrates for colloidal epitaxy: (a) bitmap pattern of a $40 \times 40$ square array, (b) schematic view of focused ion beam (FIB) milling to create patterned features, (c) SEM image of as-patterned glass substrate, (d) AFM image of representative region of as-patterned substrate, (e) AFM image of representative patterned region after etching for 30 s. in a hydrofluoric acid solution (5 volume %), and (f) SEM image of patterned and etched glass substrate comprised of dimpled features that are 400 nm in depth with a 1.21 μm pitch.[34]

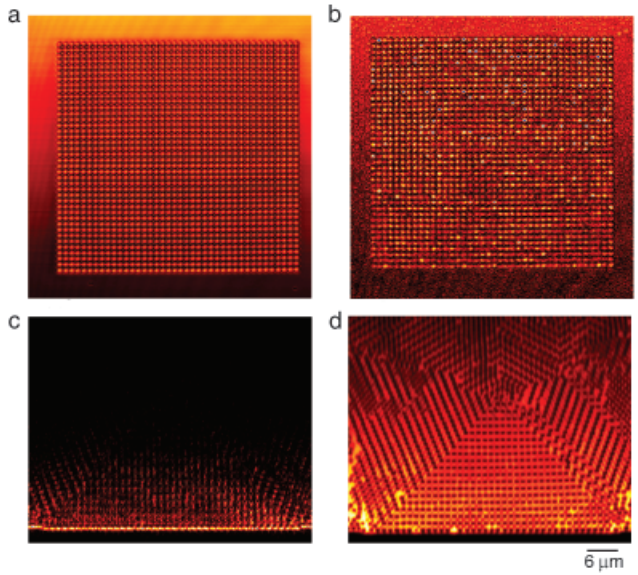


**Fig. 10.** Confocal images of epitaxial patterning of colloidal microspheres assembled from binary mixtures ($\phi_{micro} = 10^{-3}$ $\phi_{nano} \sim 3 \times 10^{-4}$): (a) *x–y* scan of the initial patterned substrate, (b) *x–y* scan of the patterned substrate after 18 min of microsphere sedimentation, (c) *x–z* scan of sediment in aqueous solution,[33] and (d) *x–z* scan of sediment after gelling, drying, and infiltration with an index-matched solution containing fluorescent dye, where dark circular features correspond to individual microspheres and bright features correspond to the dyed solution.[33]

solution. Zhu *et al.*[32] have recently demonstrated that the stability of single-wall carbon nanotubes (SWNT) in aqueous solution can be regulated by the addition of highly positively charged, hydrous zirconia nanoparticles. Interestingly, these negligibly charged SWNTs species are highly anisotropic with one dimension on the order of the nanoparticle species size. Hence, they differ fundamentally from the equiaxed microspheres studied previously. Taken as a whole, these recent observations suggest that nanoparticle haloing offers a broadly applicable, new route for controlling the stability, structure, and properties of colloidal suspensions.

Several efforts are underway to exploit the nanoparticle-mediated assembly of colloidal crystals,[7,18,33] granules, and films, and the future outlook is bright. As one example, Lee *et al.*[33] have created colloidal crystals with defined orientation by a nanoparticle-mediated, epitaxial assembly route. Specifically, focused ion beam (FIB) milling was used to produce a square array of patterned features on a glass substrate, as shown in Fig. 9. A bitmap pattern directs the rastered ion beam motion to create a series of dimpled features on a glass substrate. Subsequent milling of the substrate surface removes milling debris, and enlarges and smoothes the patterned features. In the example shown in Fig. 9, the final pattern consists of a $40 \times 40$ square array of dimples with a hole depth of 400 nm and pitch of 1.21 μm. Individual microspheres are then settled from a dilute microsphere–nanoparticle mixture ($\phi_{micro} = 10^{-3}$ and $\phi_{nano} \sim 3 \times 10^{-4}$) comprised of silica microspheres of average radius $0.59 \pm 0.01$ μm and hydrous zirconia nanoparticles of average radius 3 nm onto these patterned features and imaged in situ using confocal microscopy, as shown in Fig. 10. Individual colloidal microspheres settle into the dimpled features after several minutes. After complete sedimentation (>several hours), the sample is imaged in the *x–z* plane. It is difficult to resolve individual microspheres because of the refractive index mismatch between the colloids and the aqueous solution in which they reside. After gelling the surrounding nanoparticle solution by raising pH, the sample can then be dried and infiltrated with an index-matched glycerol–water solution that contains fluorescent dye. Confocal microscopy reveals the existence of an epitaxially templated (100 fcc) colloidal crystal above the patterned region, which is robust enough to withstand both drying and subsequent infiltration.

In summary, the ability to tailor the phase behavior, structure, rheology, and assembly of colloidal suspensions through the addition of highly charged nanoparticles has been demonstrated. The concept of "nanoparticle engineering" opens up new avenues for the processing of advanced ceramic materials from colloidal building blocks. We are now developing new approaches that exploit this novel system behavior, including both patterning of colloid–nanoparticle films via evaporative lithography and colloidal granules via microfluidic-based assembly.

## Acknowledgments

We gratefully acknowledge V. Tohver Milam, C.J. Martinez, A.T. Chan, J. Liu, W. Lee, E. R. Weeks, P.V. Braun, E. Luijten, and K.S. Schweizer for their valuable contributions to this work. The authors also acknowledge the use of the facilities at the Center for Microanalysis of Materials housed with the Frederick Seitz Materials Research Laboratory at the University of Illinois at Urbana-Champaign.

## References

[1]F. F. Lange, "Powder Processing Science and Technology for Increased Reliability," *J. Am. Ceram. Soc.*, **72** [1] 3–15 (1989).
[2]J. A. Lewis, "Colloidal Processing of Ceramics," *J. Am. Ceram. Soc.*, **83** [10] 2341–59 (2000).
[3]I. A. Aksay, "Microstructure Control Through Colloidal Consolidation"; pp. 94–104 in *Advances in Ceramics, Vol. 9, Forming of Ceramics*, Edited by J. A. Mangels, and G. L. Messing. American Ceramic Society, Columbus, OH, 1984.
[4]J. Guo and J. A. Lewis, "Effects of Ammonium Chloride on the Rheological Properties and Sedimentation Behavior of Aqueous Silica Suspension," *J. Am. Ceram. Soc.*, **82** [9] 2345–58 (1999).
[5]F. H. Norton, *Elements of Ceramics*, 2nd edition, pp. 1–5. Addison-Wesley, Reading, MA, 1974.
[6]V. Tohver, J. E. Smay, A. Braem, P. V. Braun, and J. A. Lewis, "Nanoparticle Halos: A New Colloid Stabilization Mechanism," *Proc. Natl. Acad. Sci.*, **98** [16] 8950–4 (2001).
[7]V. Tohver, A. Chan, O. Sakurada, and J. A. Lewis, "Nanoparticle Engineering of Complex Fluid Behavior," *Langmuir*, **17** [26] 8414–21 (2001).
[8]S. Asakura and F. Oosawa, "Interaction between Particles Suspended in Solutions of Macromolecules," *J. Polymer Sci.*, **33**, 183–92 (1958).
[9]A. Vrij, "Polymers at Interfaces and the Interactions in Colloidal Dispersion," *Pure Appl. Chem.*, **48**, 471–83 (1976).
[10]J. F. Joanny, L. Leibler, and P. G. de Gennes, "Effects of Polymer Solutions on Colloid Stability," *J. Polym. Sci. Polym. Phys. Ed.*, **17**, 1073–84 (1979).
[11]A. P. Gast, C. K. Hall, and W. B. Russel, "Phase Separations Induced in Aqueous Colloidal Suspensions by Dissolved Polymer," *Faraday Discuss. Chem. Soc.*, **76**, 189–201 (1983).
[12]J. F. Gilchrist, A. T. Chan, E. R. Weeks, and J. A. Lewis, "Phase Behavior and 3D Structure of Strongly Attractive Microsphere–Nanoparticle Mixtures," *Langmuir*, **21** [24] 11040–7 (2005).
[13]A. T. Chan and J. A. Lewis, "Electrostatically Tuned Interactions in Silica Microsphere–Polystyrene Nanoparticle Mixtures," *Langmuir*, **21** [19] 8576–9 (2005).
[14]F. Caruso, R. A. Caruso, and H. Mohwald, "Nanoengineering of Inorganic and Hybrid Hollow Spheres by Colloidal Templating," *Science*, **282**, 1111–4 (1998).
[15]K. J. Konsztowicz and R. Langlois, "Effects of Heteroflocculation of Powders on Mechanical Properties of Zirconia Alumina Composites," *J. Mater. Sci.*, **31** [6] 1633–41 (1996).
[16]A. Bleier and E. Matijevic, "Heterocoagulotion. I. Interactions of Monodispersed Chromium Hydroxide with Polyvinyl Chloride Latex," *J. Colloid Interface Sci.*, **55** [3] 510–24 (1976).
[17]J. Y. Walz and A. Sharma, "Effect of Long Range Interactions on the Depletion Force between Colloidal Particles," *J. Colloid Interface Sci.*, **168**, 485–96 (1994).
[18]C. J. Martinez, J. W. Liu, S. K. Rhodes, E. Luijten, E. R. Weeks, and J. A. Lewis, "Interparticle Interactions and Direct Imaging of Colloidal Phases Assembled from Microsphere–Nanoparticle Mixtures," *Langmuir*, **21** [22] 9978–89 (2005).
[19]T. T. Nguyen, A. Y. Grosberg, and B. I. Shklovskii, "Macroions in Salty Water with Multivalent Ions: Giant Inversion of Charge," *Phys. Rev. Lett.*, **85**, 1568–71 (2000).
[20]R. Garibay-Alonso, J. M. Mendez-Alcaraz, and R. Klein, "Phase Separation of Binary Liquid Mixtures of Hard Spheres and Yukawa Particles," *Physica A (Amsterdam)*, **235**, 159–69 (1997).
[21]P. G. Ferreira, M. Dymitrowksa, and L. Belloni, "Mixtures of Charged Colloids and Nonadsorbing Flexible Polyelectrolytes: An Integral Equation Study," *J. Chem. Phys.*, **113**, 9849–62 (2000).
[22]S. Karanikas and A. A. Louis, "Dynamic Colloidal Stabilization by Nanoparticle Halos," *Phys. Rev. Lett.*, **93** [24] (2004) Art. No. 248303.
[23]J. Liu and E. Luijten, "Stabilization of Colloidal Suspensions by Means of Highly Charged Nanoparticles," *Phys. Rev. Lett.*, **93** [24] (2004) Art. No. 247802.

[24]J. Liu and E. Luijten, "Colloidal Stabilization via Nanoparticle Haloing," *Phys. Rev. E*, **72** (2005) Art. No. 061401.
[25]J. Israelachvili, *Intermolecular & Surface Forces*, 2nd edititon, Academic Press, London, 1991.
[26]R. J. Hunter, *Foundations of Colloid Science*, 2nd edititon, Oxford University Press, New York, 2001.
[27]D. C. Prieve and W. B. Russel, "Simplified Predictions of Hamaker Constants from Lifshitz Theory," *J. Colloid Interface Sci.*, **125**, 1–13 (1988).
[28]R. Hogg, T. W. Healy, and D. W. Fuerstenau, *Trans. Faraday Soc.*, **62**, 1638–51 (1966).
[29]J. E. Sader, S. L. Carnie, and D. Y. Chan, "Accurate Analytic Formulas for the Double-Layer Interaction between Spheres," *J. Colloid Interface Sci.*, **171**, 46–54 (1995).
[30]S. Asakura and F. Oosawa, "On Interaction between Two Bodies Immersed in a Solution of Macromolecules," *J. Chem. Phys.*, **22**, 1255–56 (1954).
[31]D. Kong, H. Yang, Y. Yang, S. Wei, J. Wang, and B. Cheng, "Dispersion Behavior and Stabilization Mechanism of Alumina Powders in Silica Sol," *Mater. Lett.*, **58** [27–28] 3503–8 (2004).
[32]J. Zhu, M. Yudasaka, M. F. Zhang, and S. Iijima, "Dispersing Carbon Nanotubes in Water: A Noncovalent and Nonorganic Way," *J. Phys. Chem. B.*, **108** [31] 11317–20 (2004).
[33]W. Lee, A. Chan, M. A. Bevan, J. A. Lewis, and P. V. Braun, "Nanoparticle-Mediated Epitaxial Assembly of Colloidal Crystals on Patterned Substrates," *Langmuir*, **20** [13] 5262–70 (2004).
[34]C. J. Martinez and J. A. Lewis. unpublished work. □